

Geomechanical Characterization and Stability Analysis of the Bedrock Underlying the Costa Concordia Cruise Ship

Giulia Dotta¹ · Giovanni Gigli¹ · Federica Ferrigno¹ · Giuliano Gabbani¹ ·
Massimiliano Nocentini¹ · Luca Lombardi¹ · Andrea Agostini¹ · Teresa Nolesini¹ ·
Nicola Casagli¹

Received: 23 May 2016 / Accepted: 8 April 2017 / Published online: 9 May 2017
© The Author(s) 2017. This article is an open access publication

Abstract The shipwreck of the Costa Concordia cruise ship, which ran aground on 13 January 2012 on the northwestern coast of Giglio Island (Italy), required continuous monitoring of the position and movement of the vessel to guarantee the security of workers and rescuers operating around and within the wreck and to support shipwreck removal operations. Furthermore, understanding the geomechanical properties and stability behaviour of the coastal rock mass and rocky seabed underlying the ship was of similar importance. To assess the stability conditions of the ship, a ground-based monitoring system was installed in front of the wreck. The network included a terrestrial laser scanner (TLS) device, which was used to perform remote semiautomatic geomechanical characterization of the observed rock mass. Using TLS survey techniques, three main discontinuity sets were identified in the granitic rock mass of Giglio Island. Furthermore, a multibeam bathymetric survey was used to qualitatively characterize the seabed. To integrate the processed TLS data and quantitatively describe the rock mass quality, a subsequent field survey was carried out to provide a rock mass geomechanical evaluation (from very good to moderate quality). Based on the acquired information, kinematic and stability analyses were performed to create a spatial prediction of rock failure mechanisms in the study area. The obtained kinematic hazard index values were generally low; only the plane failure index reached slightly higher values. The general stability of the rock mass was

confirmed by the stability analysis, which yielded a high safety factor value (approximately 12).

Keywords Risk management · Laser scanning · Geomechanical characterization · Displacement monitoring · Stability analysis · Giglio Island

1 Introduction

On the night of 13 January 2012, the Costa Concordia cruise ship changed her original course, sailed close to the coast of Giglio Island (Tuscany, Italy), and crashed on the underwater rock of Le Scole, approximately 800 m south of the port entrance (Giglio Porto) on the east coast of the island (Schröder-Hinricks et al. 2012). The impact produced a 70-m-long gash on the left side of the hull (Fig. 1c). Immediately, sea water started to flood the engine room, gradually inundating the ship and causing a blackout. The ship began to drift backward and to port, following a 180° rotation driven by inertia and wind. One hour after the collision, the ship lay on its starboard side at an angle of more than 50° in its final position on the granitic seabed in front of Punta Gabbianara, a portion of coast located north of Giglio Porto (Fig. 1b).

Soon after the shipwreck, the search and rescue (SaR) operations for people involved in the tragedy started, coordinated by the Italian fire brigade and coast guard. The SaR operations were performed in difficult and dangerous conditions. Unfortunately, among the 4200 passengers onboard (3206 passengers and 1023 crew and personnel), a total of 32 people were killed. The final position of the cruise ship made the SaR operations more difficult due to its precarious position between two granitic prominences on a seabed sloping at 22°.

✉ Giulia Dotta
giulia.dotta@unifi.it

¹ Department of Earth Sciences, University of Firenze, via La Pira 4, 50121 Florence, Italy

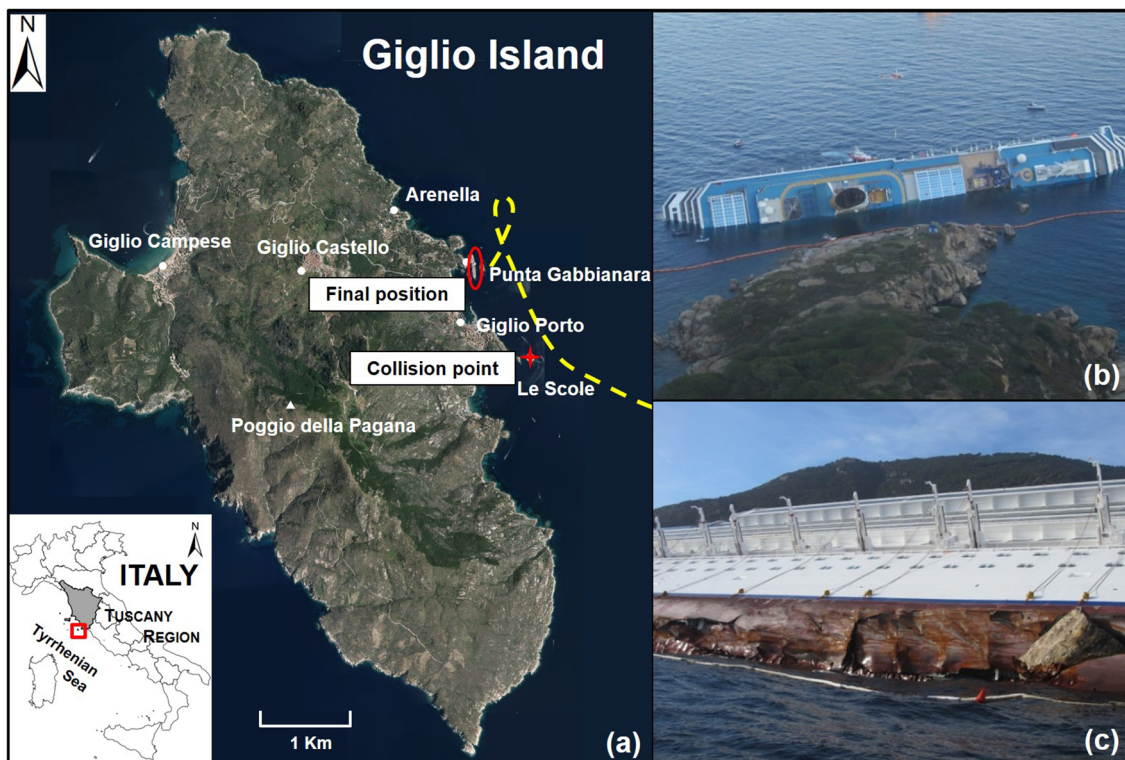


Fig. 1 a Giglio Island (Tuscany/Central Italy, Italy). The route (yellow dashed line), collision point (red cross) and final position of the cruise ship (red oval) are indicated; b view of final position of

Costa Concordia vessel; c view of 70-m-long gash on left side of hull (colour figure online)

On 20 January 2012, the Italian Council of Ministers officially declared a national state of emergency on Giglio Island, and the head of the civil protection department (DPC) was appointed delegate commissioner by an ordinance of the prime minister. To ensure the safety of the personnel involved in the SaR operations, continuous surveillance of the potential movement of the wreck was considered necessary, and the DPC requested a sophisticated ground-based real-time warning system, which was installed on Punta Gabbianara. In the very first phase of the emergency, nine different technologies were used to measure different components of the ship movement (Fig. 2): two onboard accelerometers, two robotic total stations, a ground-based Synthetic Aperture Radar (SAR) interferometer (Broussolle et al. 2014), satellite SAR sensors, a Terrestrial Laser Scanner (TLS), three microseismic stations, a Global Positioning System (GPS) antenna and receivers, an underwater extensometer and underwater markers. Moreover, Constellation of Small Satellites for Mediterranean basin Observation (COSMO) Sky-Med images were acquired (Raspini et al. 2014).

The employed system was able to record every movement and deformation endured by the wreck during the 2.5 years it remained on Punta Gabbianara. Furthermore, during the most critical phases, i.e. the fuel removal and

refloating operations (the uprighting of the ship, i.e. par-buckling, on 14 July 2014), the system was used to ensure the safety of the operations and the security of the personnel involved (Ciampalini et al. 2016). The Costa Concordia vessel, towed by two large tugboats and assisted by a suitable convoy, left Giglio Island on 23 July 2014 and arrived at the Port of Genoa on 27 July 2014, where it was dismantled.

To support removal operations and better understand the stability of the Punta Gabbianara rock mass and the underwater reef, detailed study of the geomechanical and stability behaviour was necessary. Taking advantage of the deployment of the laser scanner device for monitoring operations (Fig. 2), semiautomatic structural characterization of the TLS-observed portion of Punta Gabbianara was performed.

The terrestrial laser scanning technique is widely used for characterization and analysis of unstable slopes, as it rapidly and safely captures a highly detailed and accurate three-dimensional (3D) representation of the plano-altimetric morphology and geostructural setting of the investigated rock mass (Abellan et al. 2006, 2010; Fanti et al. 2012; Gigli et al. 2009, 2012a, b; Jaboyedoff et al. 2009; Lombardi et al. 2006; Oppikofer et al. 2009; Rahman et al. 2006; Slob et al. 2002; Slob and Hack 2004, 2007; Tapete

Fig. 2 Monitoring system locations: seismometers (green dots), terrestrial laser scanner (purple dot), ground-based SAR interferometer MIMO SAR (cyan blue), total stations (red dots) and benchmarks used by the total station (crossed circles), GPS (grey dot), accelerometers (yellow dots), extensometer (brown dot), spaceborne SAR COSMO Sky-MED (grey dot) (colour figure online)



et al. 2012; Turner et al. 2006). Furthermore, in recent years, many authors have worked on semiautomatic extraction of 3D rock mass properties from remotely acquired high-resolution data, mainly digital photogrammetry and Light Detection And Ranging (LIDAR) (Ferrero et al. 2009; Gigli and Casagli 2011; Jaboyedoff et al. 2007; Lato et al. 2009; Sturzenegger and Stead 2009; Slob et al. 2005).

For underwater rock mass characterization, the DPC requested that the OGS (National Institute of Oceanography and Experimental Geophysics) perform a multibeam survey to obtain a 3D representation of the seafloor surrounding the Costa Concordia cruise ship and to analyse in detail the morphological and bathymetric characteristics.

The remote survey results were subsequently integrated with a conventional geomechanical survey to characterize the whole rock mass in terms of geomechanical behaviour. Moreover, a geophysical survey obtained additional information on the rock mass quality.

All the acquired data were used to investigate the main rock failure mechanisms affecting the Punta Gabbianara rock mass and the granitic seabed and to perform a stability analysis of the investigated area.

2 Geographical and Geological Setting

Giglio Island, located in the Northern Tyrrhenian Sea, 20 km off the Tuscany coast, is the second largest island of the Tuscan Archipelago, covering an area of 21.2 km² (Fig. 1a). The island reaches a maximum altitude of

approximately 500 m at the Poggio della Pagana, which belongs to the main mountain ridge. It is bounded on the east side by gentle slopes and on the west side by steep slopes that rise abruptly from the sea to maximum elevation of several tens of metres. Flat areas are very rare and limited to recent beaches (e.g. Campese and Arenella) and some small areas located on the ridge; one exception is the Ortana Valley, situated just southwest of Campese Village.

From a geologic perspective, Giglio Island consists mainly of magmatic rocks with monzogranitic composition (average Rb/Sr radiometric age 5 Ma), representing one of the largest intrusive complexes in the Tuscan Magmatic Province. The main intrusive complex is the Giglio Monzogranite Intrusion (GMI), which is characterized by an outer zone that is extremely foliated and locally layered (Pietrabona Facies, PBF) and an inner zone that is highly porphyritic and texturally homogeneous (Arenella Facies, ARF) (Westerman et al. 1993) (Fig. 3).

The Scole Monzogranite Intrusion (SMI) is a distinctive intrusive complex that is more acidic in composition than the GMI and that has a fully exposed contact with the ARF intrusion. The SMI rocks crop out along the eastern coast of the island (Fig. 3). On Punta Gabbianara, where the vessel was beached, monzogranitic rocks belonging to the ARF intrusion crop out. According to the structure of the intrusion, the underwater bedrock could be exclusively constituted by monzogranite rocks belonging to the SMI.

The strong lithologic contrasts and large number of fractures produce different instability phenomena on the granitic slopes of the island, such as rockfall events, slides, escarpment degradation, detritus accumulation and altered deposits.

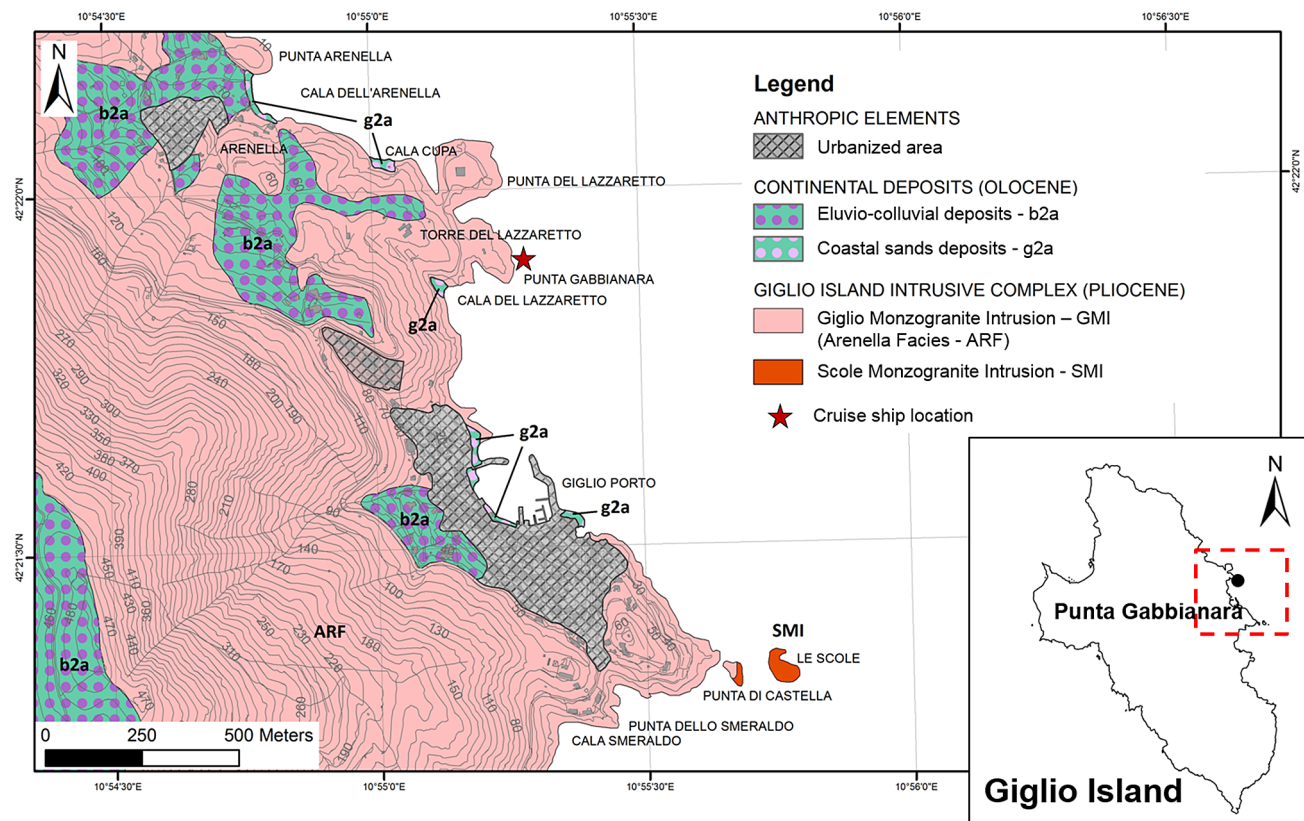


Fig. 3 Detail of Tuscany geological map 1:10,000—Giglio Island GIG(030-040-070-080) section and cruise ship location (*red star*) (colour figure online)

The monzogranite bedrock influences the erosion phenomena, and most of the sand on the island is derived from granite, forming sandstone deposits thicker than 3 m.

Weathering generates typical exfoliation, sheeting and isolated spheroidal blocks. In general, the origin of the exfoliation process in granitic rocks is mainly connected with unloading of compressive stress caused by erosion and/or by pluton expansion and cooling of the magmatic body (Blackwelder 1925). These structures are formed approximately parallel to the outer surface of the magmatic intrusion (free surface). The underwater bedrock was also likely influenced by the ascent of the magma in the pluton, leading to outcrops with exfoliation and alteration characteristics.

The landscape is characterized by well-rounded forms and bevelled edges, in some cases even on steep slopes. Locally, the surface of the granite features alveolar and tafoni shapes.

3 Data Collection

3.1 Laser Scanning and Multibeam Surveys

Long-range TLS technology can generate a high-resolution 3D point cloud by measuring the scanner–object distance with centimetre accuracy by calculating the round-trip time

of a laser pulse (with near-infrared wavelength) to reach the object surface from the point of emission and return. These point clouds can then be used for construction of 3D models.

On the first day of monitoring activity, a fixed long-range 3D laser scanner (RIEGL LMS-Z410i) was installed in the vicinity of Punta Gabbianara, precisely at Torre del Lazzaretto (Fig. 2), to remotely detect displacement of the Costa Concordia. This device is able to determine the position of up to 12,000 points per second, with maximum angular resolution of 0.008° and accuracy of ± 10 mm (one σ at 50-m range under RIEGL test conditions) from a maximum distance of 800 m.

The location of the RIEGL LMS-Z410i allowed us to observe a portion of the rock mass (Fig. 2) and to rapidly acquire detailed information on inaccessible rock outcrops, thereby minimizing survey time in this emergency situation.

The acquired 3D point cloud of the investigated area was cleared of vegetation and linked to a global reference system with the aid of reference points with coordinates defined using a differential GPS.

Using the high-resolution point cloud obtained by the TLS, an accurate remote semiautomatic geomechanical survey was possible. In this case, semiautomatic extraction of the main geomechanical characteristics of the rock mass

discontinuities was performed using a MATLAB tool called DiAna (discontinuity analysis) (described in detail in Gigli and Casagli 2011). This tool allows the user to investigate geometric parameters suggested by the International Society for Rock Mechanics (1978), such as orientation, number of sets, spacing, persistence, block size and scale-dependent roughness.

DiAna is based on definition of least-squares fitting planes on clusters of points extracted by moving a sampling cube on an unorganized point cloud. By selecting the cube size and a standard deviation threshold, it is even possible to investigate rock masses characterized by highly irregular block shapes. The geometrical properties can be calculated, and the search cube dimensions are based on the TLS data resolution and the size of the features considered. The cluster is considered valid if the associated standard deviation is below a defined threshold.

The cluster orientations are plotted on a stereographic projection, and the sets of the main discontinuity planes can be identified and extracted from the cloud.

Moreover, by drawing on the point cloud a cylinder with axis perpendicular to the plane of each discontinuity passing through the centroid and base containing the surface points, it is possible to count the number of discontinuities intersected by the cylinder and associated with the same set. This process can be used to assess the true spacing and frequency of discontinuity sets for three-dimensional data.

Semiautomatic analysis was carried out on the investigated portion of Punta Gabbianara rock mass, while manual extraction was performed for the shadow regions. The poles of the semiautomatically extracted discontinuities are presented in a stereographic projection in Fig. 4.

Three sets of discontinuities were recognized: a low-dip-angle set JN1 ($229^\circ/29^\circ$) and two high-dip-angle sets JN2 ($281^\circ/83^\circ$) and JN3 ($340^\circ/86^\circ$) (Table 1). The true spacing was approximately 3 m for sets JN1 and JN2 and approximately 3.2 for discontinuity set JN3.

Furthermore, a bathymetric survey was carried out by the OGS of Trieste (Italy) on 22 January 2012 using the high-frequency acoustic wave pulse technique to survey the seafloor in detail. The device employed was a Reson SeaBat 8125 multibeam echosounder based on the high-frequency acoustic wave pulse technique. This sonar system produces 240 beams with frequency of 455 kHz, swath coverage of 120° , depth resolution of 6 mm, near-field resolution of 2.5 cm and maximum range of 120 m (unpublished internal report).

The multibeam data (Fig. 5) identified two rock spurs at average depth of 22 m, on which the wreck lay. The ocean bottom consisted of granitic rock with apparently good geomechanical characteristics and was continuous with the rock above sea level. These characteristics were even improved by the abrasive action of waves, which removed altered portions (unpublished internal report).

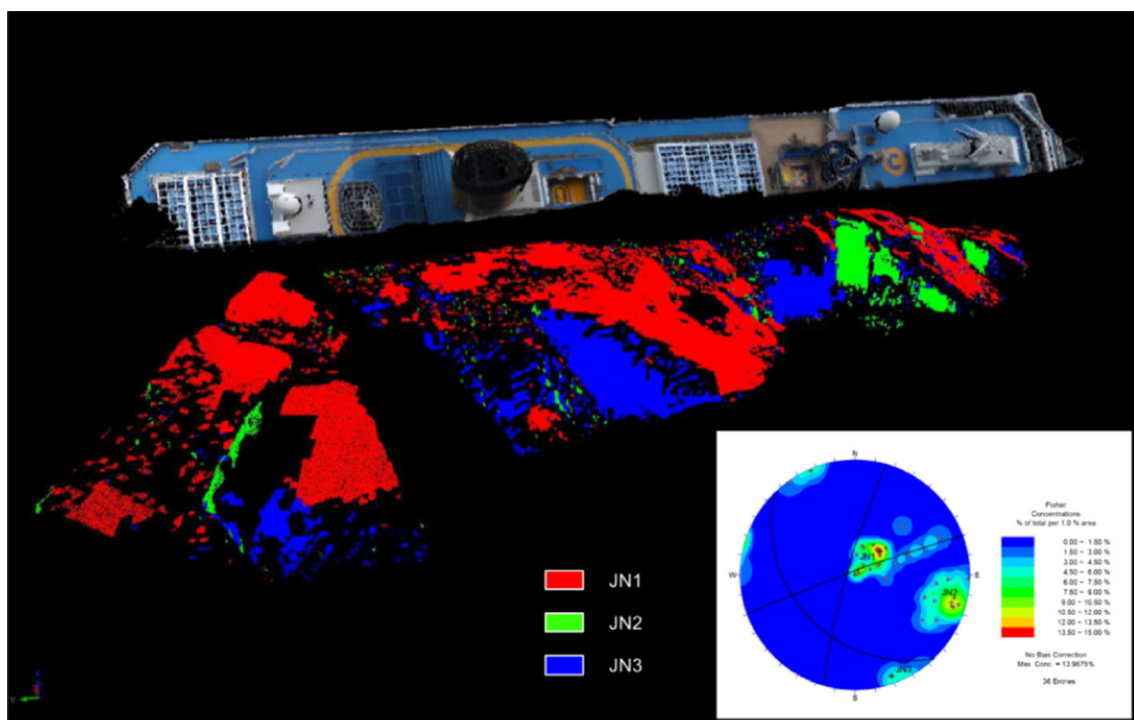


Fig. 4 3D representation of main joint sets extracted from point cloud and stereographic projection of discontinuity poles and modal planes of main sets collected by semiautomatic analysis

Table 1 Geomechanical properties of rock mass discontinuity sets obtained from traditional and laser scanning surveys

Set id	α (°)	β (°)	X (m)	JCS (MPa)	JRC	c (MPa)	Φ (°)
JN1	229	29	3	72	5	0.016	42.88
JN2	281	83	3	72	5	0.016	42.88
JN3	351	85	3.2	84	5	0.016	43.21
JN4	54	43	0.6	78	8.9	0.049	50.22
JN5	25	86	1.8	81	9.1	0.052	50.69
JN6	321	80	5.1	72	10	0.066	51.66

Set id, joint set identification code; α , dip direction; β , dip; X, true spacing; JCS, joint compressive strength; JRC, joint roughness coefficient; c, average cohesion; Φ , average friction angle

3.2 Traditional Field Survey

To integrate the semiautomatic rock mass characterization and to obtain a quantitative description of the

discontinuities of the rock mass, a traditional survey was also performed: 20 point load tests on monzogranite samples and 7 scanline surveys (varying from 20 to 33 m in length) were carried out, according to the methods suggested by ISRM (1978, 1985).

The point load tests were executed on Cala Lazzaretto samples (Fig. 5, blue dots) and on undisturbed rock to measure the tensile (σ_t) and compressive (σ_c) strength. Then, the point load strength index, σ_t and σ_c were evaluated by applying a conversion factor of 1.3 according to Johnston (1993). The resulting average values for $\sigma_{c(1)}$ and $\sigma_{t(1)}$ for the specimens sampled in the first location were 115.14 and -3.84 MPa, respectively. For the second location, were values are 111.88 and -3.73 MPa, respectively. The resulting average σ_c value of the investigated area was 113.51 MPa (DPC 2012), and this value was used to classify the rock. This value is lower than the common intact rock resistance values of granite (approximately 150 MPa, i.e., Hansen 1988; Hoek and Brown 1980), likely

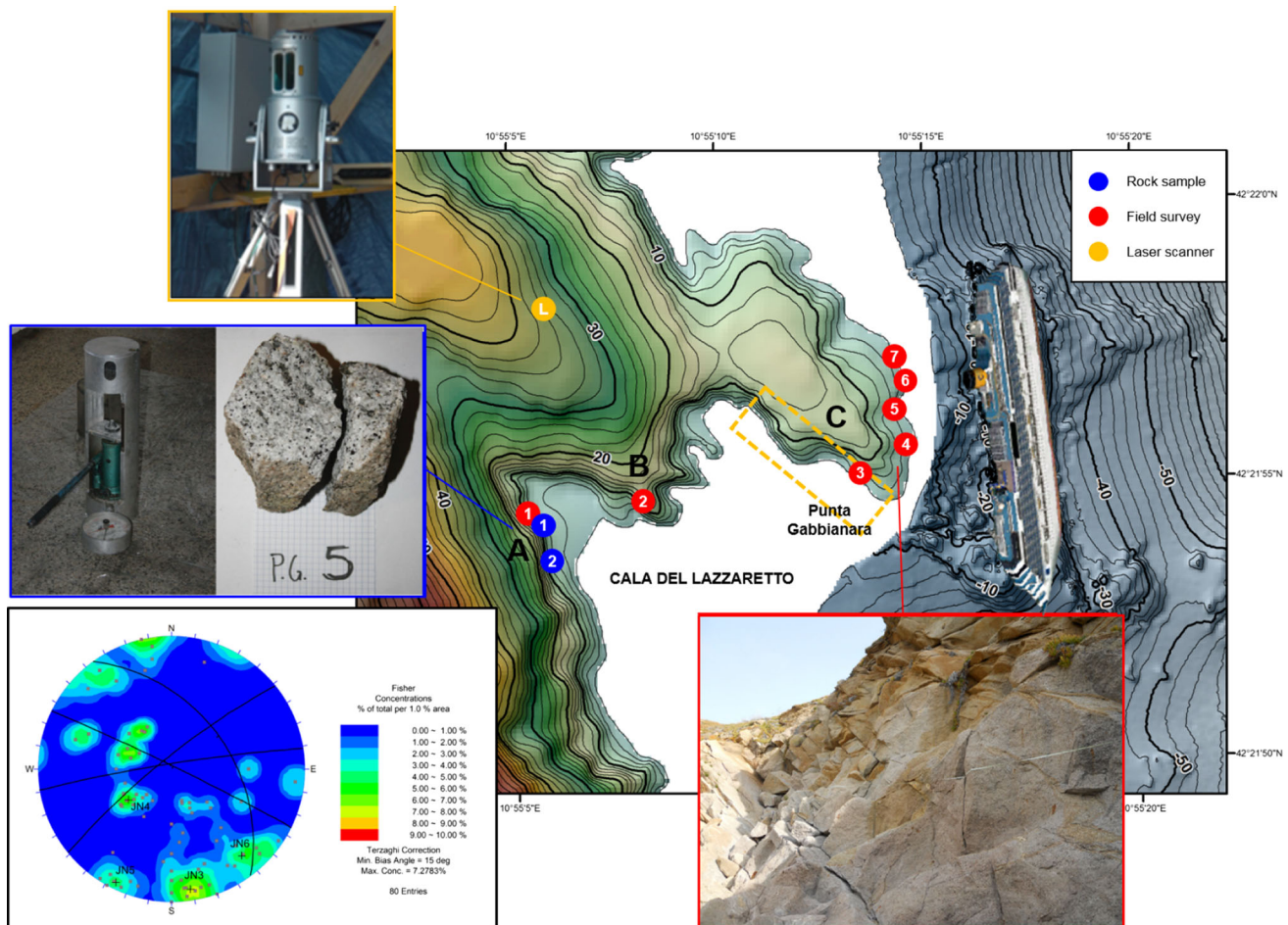


Fig. 5 Location of seven scanlines (red dots), point load tests (blue dots), terrestrial laser scanner device (yellow dot) and portion of rock mass observed by TLS device (yellow dashed rectangular) in the study area and stereographic projection of discontinuity poles and

modal planes of main sets collected by traditional field surveys in sector C. The digital terrain model of the seabed (in greyscale) was carried out by multibeam survey. Letters indicate the different sectors into which the investigated area was divided (colour figure online)

due to the alteration observed to affect the rock to depth of 1 m.

According to geologic features, the investigated site was divided into three sectors (Fig. 5):

- Sector A: unweathered rock, very low fracturing frequency
- Sector B: weathered and locally highly weathered rock (heavily broken granite), average fracturing frequency with open fractures (up to several decimetres)
- Sector C: unweathered and locally slightly unweathered rock, low fracturing frequency

The main geomechanical features (orientation, spacing, persistence, roughness, joint wall strength, aperture, filling and seepage) of discontinuities were obtained by acquisition of seven scanline surveys (Fig. 5, red dots), mainly performed on the northeastern slope of Punta Gabbianara (sector C). Furthermore, to complete the investigation of the mechanical behaviour of the area surrounding the shipwreck, random joint orientation measurements were also taken.

Since the area of interest in this work is the area around the shipwreck, the geomechanical results for sector C are reported.

In accordance with the semiautomatic analysis data, the conventional survey identified the high-dip-angle set JN3 (351°/85°). Moreover, other joint sets were identified: a main medium-dip-angle set JN4 (54°/43°) and two secondary high-dip-angle sets: JN5 (25°/86°) and JN6 (321°/80°) (Fig. 5). Terzaghi correction was applied to account for sampling bias introduced by orientation data collection along the scanline.

Table 1 summarizes the modal orientation planes and the main features of the discontinuity sets recognized in sector C.

The high-dip-angle set JN3 is characterized by joints with maximum aperture of 2 cm. Most of the discontinuities were visibly weathered and contained iron, manganese and quartz fill. The length of most fractures exceeded 10 m.

The joints belonging to set JN4 featured apertures up to several decimetres wide, and most of the discontinuities were also visibly weathered with iron and manganese fill. The persistence of the set varied between 1 and 6.5 m, and in some cases, exceeded 10 m in length. The joints of both sets mostly terminated in massive rock.

The JN5 set fractures showed aperture values on the order of a few millimetres and were characterized by iron and manganese fill. The maximum persistence reached values close to 2 m, and the joints mostly terminated in massive rock.

The discontinuities belonging to the secondary high-dip-angle set JN6 featured apertures up to 1 cm wide and

mostly terminated against other joints or beyond the outcrop; the persistence was highly variable.

To estimate the geomechanical features according to ISRM (1978, 1985), the joint compressive strength (JCS) and joint roughness coefficient (JRC) were evaluated. The JCS was evaluated using the Schmidt hammer (L-type, model Proceq) sampling technique based on the correlation between the JCS and rebound number R (Deere and Miller 1966):

$$\log_{10}(\sigma_c) = 0.00088\gamma R_{(L)} + 1.01,$$

where σ_c is the JCS in MPa, γ is the unit weight of rock in kN/m^3 , and R is the rebound number of the L-type Schmidt hammer. The JRC was quantified using a profilometer and visual comparison of the surface profile with standard profiles published by Barton and Choubey (1977). This coefficient varies from 0 for a smooth, planar surface to as high as 20 for rough surfaces.

The shear strength of the discontinuities obtained from the geomechanical field and the laser scanning surveys was calculated using the Barton–Bandis failure criterion (Barton 1973). Therefore, the following data were used as input for RocData software (Rocscience 2004):

- Basic friction angle ($\phi_b = 33^\circ$) obtained from tilt tests on four rock samples, as follows (Table 2):
- The JRC and JCS for each discontinuity set (Table 1) from traditional survey. The JRC and JCS parameter values belonging to sets JN1 and JN2 were selected as the lowest among the sets. Their true spacing was obtained from the semiautomatic analysis (cf. ‘Laser scanning survey’).
- Highest tensional stress ($\sigma_{\max} = 0.7$ MPa), which is equal to the weight of the cruise ship considering the barycentre shifted toward the prow.

The resulting geomechanical discontinuities and intact rock features were used to classify each sector of rock mass by applying the main classification systems developed by Barton et al. (1974), Bieniawski (1989) and Hoek et al. (1995).

The Q -system (Barton et al. 1974) is defined as follows:

$$Q = (RQD/J_n)(J_r/J_a)(J_w/SRF),$$

where RQD is the Deere rock quality designation (Deere 1963), J_n is the joint set number, J_r is the joint roughness

Table 2 Tilt test results on four rock samples

	Test 1	Test 2	Test 3	Test 4	Test 5	Φ_b (°)
Sample 1	30.1	32.3	32.4	31.4	32.4	31.7
Sample 2	34.5	35	31.3	33.7	33.5	33.6
Sample 3	32.3	33.2	35.4	32.3	35.9	33.8
Sample 4	32.1	32.5	34.2	34.2	32.8	33.2

number for the critically oriented joint set, J_a is the joint alteration number for the critically oriented joint set, J_w is the joint water reduction factor, and SRF is the stress reduction factor. The values of these parameters are given in specific tables.

For sector C, i.e. the sector of major concern, the chosen parameters were as follows (Table 3).

The rock mass rating (RMR) system developed by Bieniawski (1989) classifies a rock mass based on five parameters: uniaxial compressive strength (P1), RQD (P2), spacing of discontinuities (P3), condition of discontinuities (P4) and groundwater conditions (P5). The resulting RMR is obtained from the sum of these five parameters, and the value of these parameters is given by the author in specific tables.

For sector C, the parameters were as follows (Table 4).

The Geological Strength Index (GSI) classification was introduced by Hoek et al. (1992) and improved in subsequent publications (e.g., Hoek et al. 1995; Hoek and Brown 1997; Marinos and Hoek 2001). The classification is essentially qualitative and is a function of descriptions of the lithology, structure and surface conditions following specific tables. Once a GSI number is defined, it is used in conjunction with appropriate parameters to employ the Hoek and Brown failure criterion. For granitic rocks, the main references are Russo et al. (2001) and Marinos et al. (2004).

In the case of high-quality rock mass, the GSI value can be obtained from the RMR system (Hoek et al. 1995) as follows:

$$\text{GSI} = \text{RMR} - 5 \text{ (Hoek et al. 1995)}$$

The resulting value of GSI (70) is in good agreement with the GSI-based geomechanical group classification (g1 group) provided by Russo et al. (2001).

The values for each index are summarized in Table 5. Furthermore, the index values for sector A and B are provided.

Additionally, discontinuities and rock mass Mohr–Coulomb equivalent strength parameters were calculated (Tables 1, 5) to perform kinematic and stability analyses.

Table 3 Q-system parameters chosen for sector C

RQD	J_n	J_r	J_a	J_w	SRF
100	6	2	2	1	1

RQD, Deere rock quality designation; J_n , joint set number; J_r , joint roughness number for the critically oriented joint set; J_a , joint alteration number for the critically oriented joint set; J_w , joint water reduction factor; SRF, stress reduction factor

Table 4 RMR parameters chosen for sector C

P1	P2	P3	P4	P5
15	20	18	7	15

P1, uniaxial compressive strength; P2, RQD; P3, spacing of discontinuities; P4, condition of discontinuities; P5, groundwater conditions

In the case of rock mass geomechanical parameters, the Hoek and Brown failure criterion (Hoek and Brown 1980; Hoek et al. 2002), considering $m_i = 30$ for granodiorite and σ_{ci} equal to the average compressive strength obtained from the point load test (113.51 MPa), was employed.

3.3 Geophysical Survey

With the aim of increasing knowledge about the investigated rock mass quality, P-wave seismic refraction and electromagnetic surveys were also performed (DPC 2012).

Three seismic refraction scanline surveys in the Cala del Lazzaretto and Punta Gabbianara areas were carried out using a DAQlink-III digital seismograph (Fig. 6), with 24 60-Hz vertical geophones and two multipolar seismic cables with 5 m between takeouts. Generation of seismic waves was performed using an 11-kg hammer. The obtained seismic tomographies (Fig. 6) show, from top down, 1–2 m of soil and highly weathered rock (P-wave velocity less than 1000 m/s), 4–8 m of weathered monzogranite (P-wave velocity between 1000 and 2500 m/s) and intact rock (P-wave velocity greater than 2500 m/s). These results reveal rock with good and very good rock qualities starting 4–8 m below ground level.

The geoelectric survey was performed using a Geonics EM-34 with intercoil spacing of 10 m and 131 measurement points arranged in 11 arrays (Fig. 6). The maximum survey depth, according to local lithological conditions, was approximately 7–8 m. This method measures the ground conductivity of the subsurface by way of electromagnetic induction, producing contour maps of apparent conductivity by interpolation of the analysis results.

Lines of high conductivity represent possible lineations or discontinuities (Fig. 6) where rock is highly fractured and weathered. Figure 6 shows that the orientations of the discontinuities detected by the geoelectric survey and those detected in the non-stereoscopic digital orthophotos (03/03/2012) were highly congruent. Comparison between the results obtained by these two techniques is a useful tool to identify discontinuity sets. The JN3 discontinuity set was clearly observed in the satellite images and represents the most persistent set recognized by the traditional survey. This set was also identified by the laser scanning survey. Other high-dip-angle discontinuity sets (JN5 and JN6)

Table 5 Geomechanical properties of rock mass

Sector	RMR	Q	GSI	c' (MPa)	Φ' (°)	σ_{tm} (MPa)	σ_{cm} (MPa)
A	87	118.8	82	3.8	68.3	-0.97	41.7
B	62	7.4	57	1	67.1	-0.15	10.2
C	75	16.7	70	1.9	68.2	-0.39	21.3

Sector, sector identification name; RMR, rock mass rating according to Bieniawski (1989); Q , Q -index according to Barton et al. (1974); GSI, Geological Strength Index according to Hoek et al. (1995); c' , average cohesion; Φ' , average friction angle; σ_{tm} , rock mass tensile strength; σ_{cm} , rock mass compressive strength

could also be identified. The JN4 and JN1 discontinuities sets were faintly visible due to their orientation.

The highly conductive zone at the southern end of the analysed zone may be caused by seawater seepage in this area.

4 Data Analysis

4.1 Kinematic Analysis

Kinematic analysis can be used to predict the spatial distribution of rock failure mechanisms using the geometric features of the identified discontinuity sets. Many authors (Goodman 1976, 1980; Goodman and Bray 1976; Hoek 1973; Hoek and Bray 1981; John 1968; Markland 1972; Matheson 1983, 1989) have used kinematic analysis for natural and artificial rock slopes.

The analysed instability mechanisms are plane failure (PF) (Hoek and Bray 1981), wedge failure (WF) (Hoek and Bray 1981), block toppling (BT) (Goodman and Bray 1976; Matheson 1983) and flexural toppling (FT) (Goodman and Bray 1976; Hudson and Harrison 1997).

For each instability mechanism, a kinematic hazard index (introduced by Casagli and Pini 1993) was calculated based on the ratio between the number of poles N (or intersections I) lying in the critical area within the stereographic projection and the total number of poles (or intersections):

$$C_{PF} = N_{PF}/N$$

$$C_{WF} = I_{WF}/I$$

$$C_{BT} = (N_{BT}/N) \times (I_{BT}/I)$$

$$C_{FT} = N_{FT}/N$$

This analysis was performed using a MATLAB tool called DiAna-K (Gigli et al. 2012a). The diagram in Fig. 7 shows the analysis process. The slope orientation, the discontinuity surface orientations (resulting from both traditional and laser scanning survey) and the discontinuity friction angle (chosen as the lower and more precautionary angle, refer to Table 1) were considered as input parameters. The intersection lines and equivalent friction angle were calculated automatically. For each surface

orientation, the value of the kinematic hazard index is obtained as an xlt, txt, stl or dip file (the file extension changing depending on the type of analysis and input files).

The program can be used to perform 3D kinematic analysis using the surface mesh (stl file) obtained from laser scanning data.

In this case, 3D analysis was performed using laser scanning data in conjunction with a regional technical map (CTR) at scale of 1:2000 because the laser scanner device only observed a limited portion of the investigated area. The data were homogeneously resampled with resolution of 0.50 m. The bathymetric survey was provided by the OGS (National Institute of Oceanography and Experimental Geophysics) of Trieste (see Subsection 3.1). In Fig. 8, the local slope orientations (dip and dip direction) are shown.

The obtained 3D kinematic analysis results (Fig. 9) show the distribution of the kinematic hazard index values of the surface of the mesh for each instability mechanism in the Punta Gabbianara and Cala del Lazzaretto areas. The probability of occurrence for each mechanism is expressed using a colour scale, varying from light green to deep red as the hazard increases, and the indexes are expressed in percent. The maximum index value is 12 %, being related to plane failure (PF, Fig. 9a), which mainly affects Cala del Lazzaretto, and to flexural toppling (FT, Fig. 9d), which mainly affects Punta Gabbianara. Both mechanisms also affect the underwater granitic reef but to a lesser extent. Wedge failure (WF, Fig. 9b) and block toppling (BT, Fig. 9c) represent negligible kinematic hazards.

Additionally, global kinematic analysis was performed (Fig. 10) to analyse in depth the kinematic hazard index values of the granitic reef underlying the cruise ship. Detailed analysis for each possible slope dip and dip direction value (varying from 0° to 90° and 0° to 360°, respectively, in an array with interval of 1°) was performed, and the average slope orientation (075°/18° with range of 30° for both coordinates) for the granitic reef underlying the cruise ship specified. The mean slope orientation of the rocky spur was obtained by computing the dip and dip direction of the triangles of the mesh using DiAna.

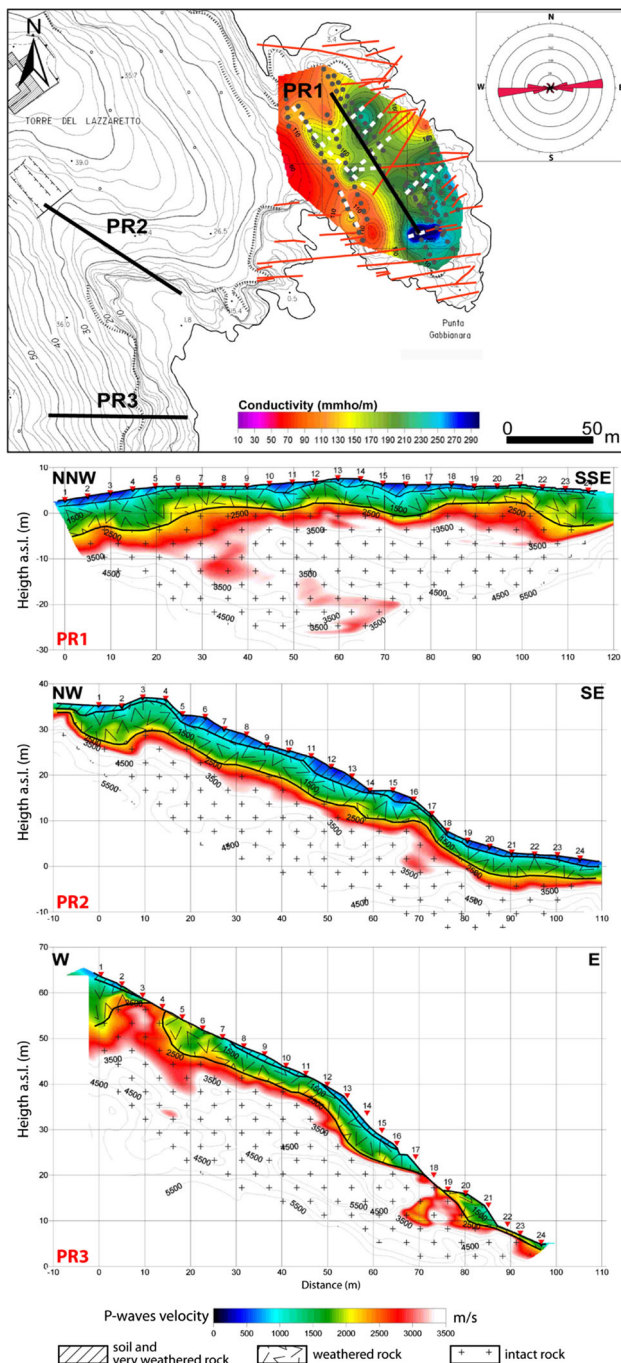


Fig. 6 *Top*: location of seismic refraction scanline surveys (black lines) and measurement points of geoelectric survey (grey dots) on the regional technical map (CTR) at scale of 1:2000 ('Carta tecnica della Regione Toscana', sheet 02/14), and apparent electromagnetic conductivity map (DPC 2012). White dashed lines indicate lineations or discontinuities hypothesized based on electromagnetic survey results; red lines: discontinuities recognized by satellite images analysis; the rosette plot of the orientation of these discontinuities is illustrated in the inset (data weighted by discontinuity trace length). *Bottom*: seismic tomography for scanlines PR1, PR2 and PR3. Weathered soil and rock are identified for each scanline (colour figure online)

This analysis confirmed that the highest kinematic index (approximately 16 %) was related to plane failure (PF, Fig. 10a) and flexural toppling (FT, Fig. 10d). The slope on which the cruise ship was stranded (red dashed line in Fig. 10) showed very low index values (5 %).

4.2 Stability Analysis

The rock mass features were reproduced using a distinct element method numerical model to study the stability of the investigated rock slope altered by the load of the shipwreck. For this purpose, the Universal Distinct Element Code (UDEC, Itasca 2004) was employed.

Since discontinuities play a significant role on the considered slope scale, use of a discontinuous method seemed most suitable. Numerical modelling was performed along a profile involving the rock mass of Punta Gabbianara (Fig. 8) above and below sea level and considering the higher slope gradients.

According to the apparent orientation of the discontinuities surveyed along the chosen profile, two main joint sets were detected: a first family of discontinuity sets (JN1 and JN4) with sub-horizontal dip angle, and a second family (JN2, JN3, JN5 and JN6) with inclination of 80°.

The block was subdivided into a mesh of finite difference elements (Fig. 11a), and for each element a Mohr–Coulomb constitutive model was assigned. Joints were assigned based on the joint area contact—Coulomb slip criterion, which assigns values of the elastic stiffness; frictional, cohesive and tensile strengths; and dilation characteristics to each joint.

Both the material and joint properties were selected based on the geomechanical survey results (Tables 1, 5). As a precautionary measure, the lowest values (weathered rock) confirmed by the point load tests and seismic refraction survey results for the shallow level of soil were used for the parameters in the modelling.

The first step of the model consisted of establishing the stress state. By assigning high strength values to materials and discontinuities and using the real elastic properties, the model converged to equilibrium under its own weight. The water table and boundary conditions were also provided, and the model still converged to a stable state (Fig. 11b). During this phase, the load exerted by the shipwreck was not yet considered. After assigning real peak strength properties to zones and joints (second step), the model still converged to a stable state, but with some deformations below the rock plate (Fig. 11c).

The subsequent step, in which the shipwreck load (7×10^5 Pa) was considered, also converged to a stable state. Some plastic deformation was obtained

Fig. 7 Flowchart of DiAna-K analysis process

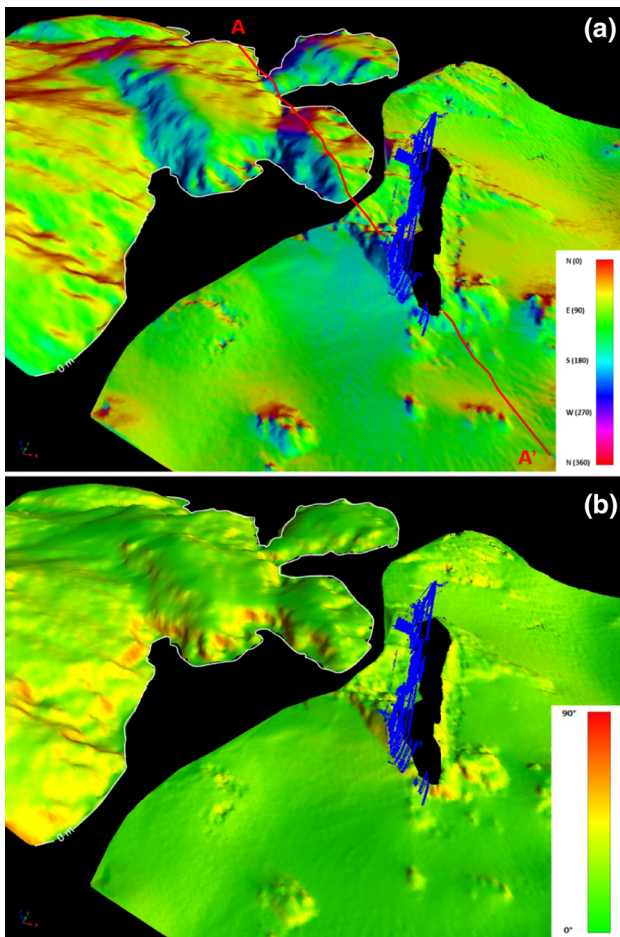
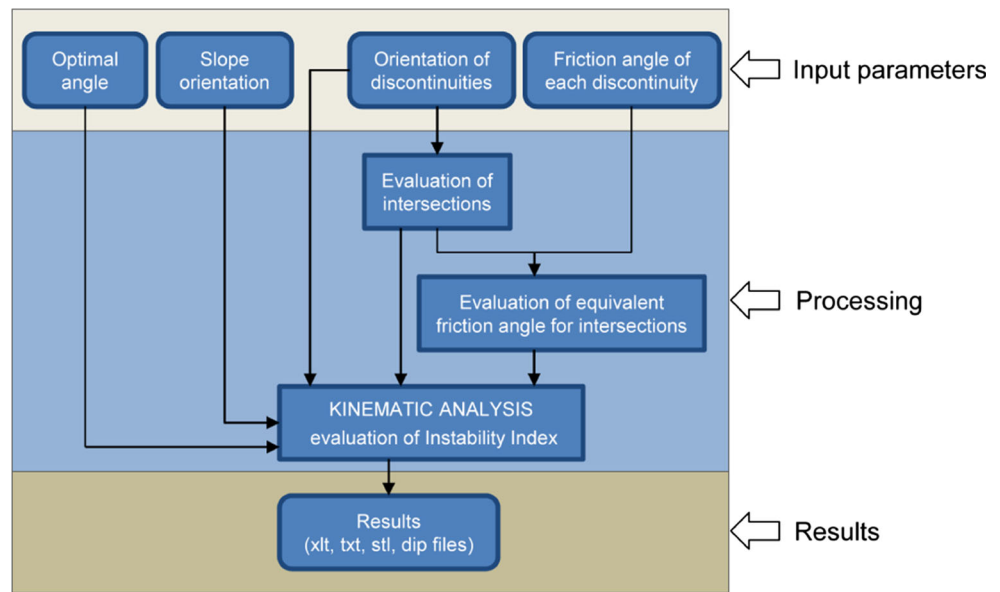


Fig. 8 3D surface mesh with distribution of rock mass dip direction (a) and dip (b) values calculated and extracted by processing 3D laser scanner data. The point cloud of the shipwreck is shown in blue. The cross-section (AA') of the study area is shown in red (colour figure online)

(Fig. 11d). With maximum displacement values of approximately 10 mm, the modelled area can be considered stable.

To obtain the SF value during the last phase, strength reduction values were assigned to both the rock mass and joint sets. The strength reduction method (Dawson et al. 1999; Griffiths and Lane 1999; Eberhardt et al. 2004) usually implements simultaneous reduction of the cohesion and friction angle parameter; in this case, the tensile strength was considered too.

The output of the stability analysis model provided the shear displacements of the joints (Fig. 12a) and the velocity vector distribution during a collapse (Fig. 12b). The safety factor value was much higher than 1 (approximately 12).

5 Discussion and Conclusions

Following the shipwreck of the Costa Concordia vessel, a real-time monitoring system was installed, and in-depth geomechanical characterization and stability analysis of the coastal rock mass and underwater seabed underlying the cruise ship performed to aid the SaR and refloating operations.

A terrestrial laser scanner (RIEGL LMS-Z410i) and other ground-based monitoring systems were installed on Punta Gabbianara (Fig. 2) in front of the wreck to detect any potential displacement of the cruise ship. From its location, the TLS was able to observe the southwestern portion of the Punta Gabbianara coastal rock mass and rapidly acquire a detailed 3D representation of the study

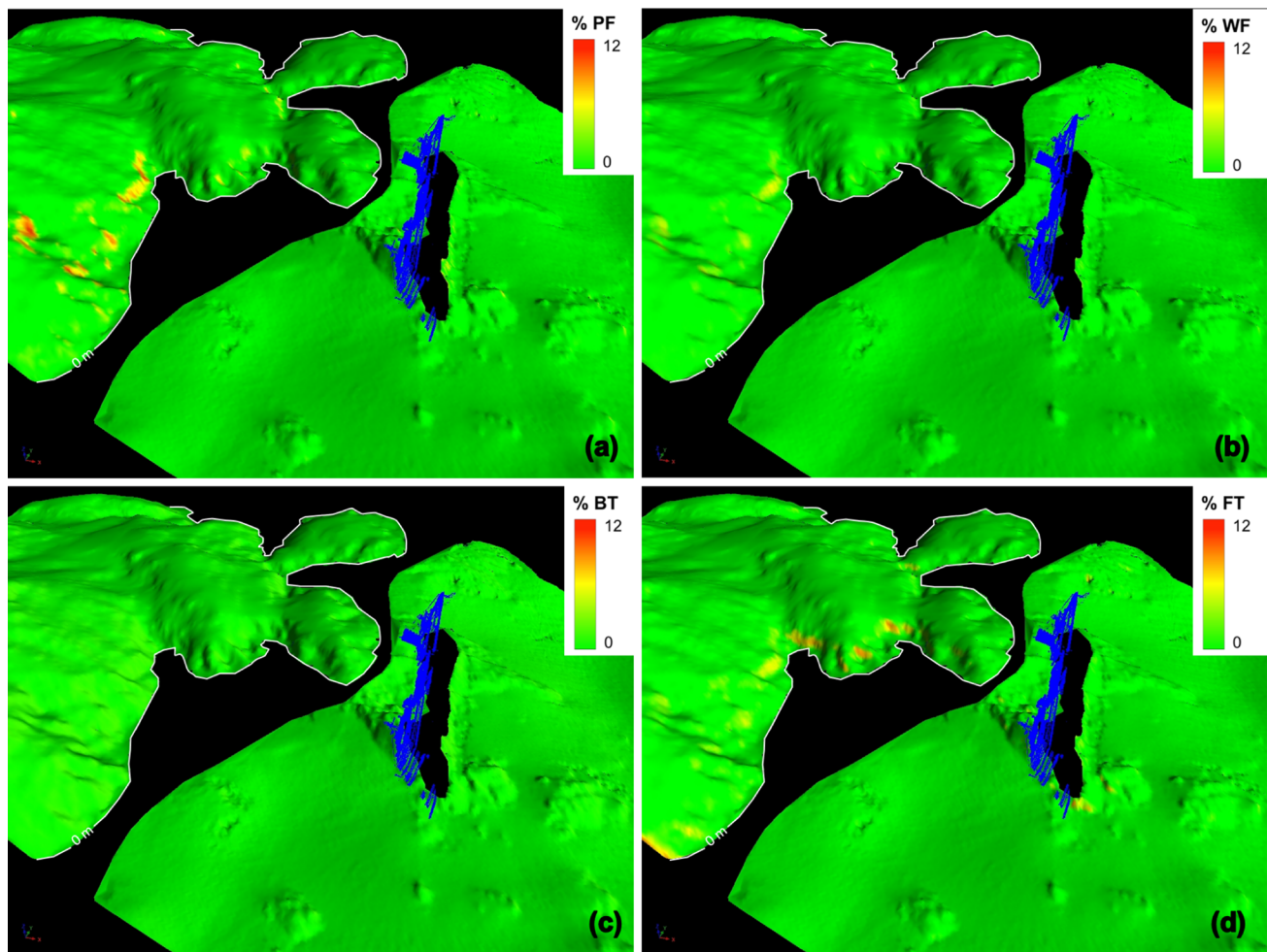


Fig. 9 Results obtained from 3D kinematic analysis for different analysed failure mechanisms (corresponding index values expressed in percent): **a** plane failure, **b** wedge failure, **c** block toppling,

d flexural toppling. The point cloud of the shipwreck is shown in *blue* (colour figure online)

area (Fig. 5). Semiautomatic extraction of the main geostructural features of the discontinuities (orientation and spacing) within the observed rock mass was performed using the MATLAB tool DiAna (discontinuity analysis) (Gigli and Casagli 2011). The clustering process recognized a low-dip-angle set (JN1) and two high-dip-angle sets (JN2 and JN3).

Furthermore, a multibeam bathymetric survey was carried out by the OGS (National Institute of Oceanography and Experimental Geophysics) of Trieste (Italy), providing a three-dimensional representation of the submerged rock mass.

A traditional field survey provided data for geomechanical reconstruction of the Punta Gabbianara rock mass and integration with the TLS characterization results. Twenty point load tests on monzogranitic samples were carried out to characterize the intact rock, and seven scanlines were performed in the study area, mainly on the northeastern slope (sector C, Fig. 5), to quantitatively describe the main features of the discontinuities according

to the methods suggested by ISRM (1978, 1985) (Table 1). Again, the JN3 discontinuity set was detected. Additionally, two other high-dip-angle sets (JN5 and JN6) and a medium-dip-angle set (JN4) were identified.

Compared with a traditional survey, semiautomatic extraction of the orientation of planes in the point cloud tended to overestimate the discontinuity sets parallel to the slope, such as set JN1, which is parallel to the slope of the southwestern region.

Sets JN5 and JN6 were probably not recognized by the semiautomatic approach because of the presence of some shadow areas in the TLS data. Occlusions in laser scanner data are a common problem due to data acquisition from a single scan location (Lato et al. 2010).

Therefore, the TLS remote survey produced satisfactory characterization of the geometric features of the discontinuity sets. Furthermore, the combination of traditional and semiautomatic survey techniques was able to characterize the whole rock exposure.

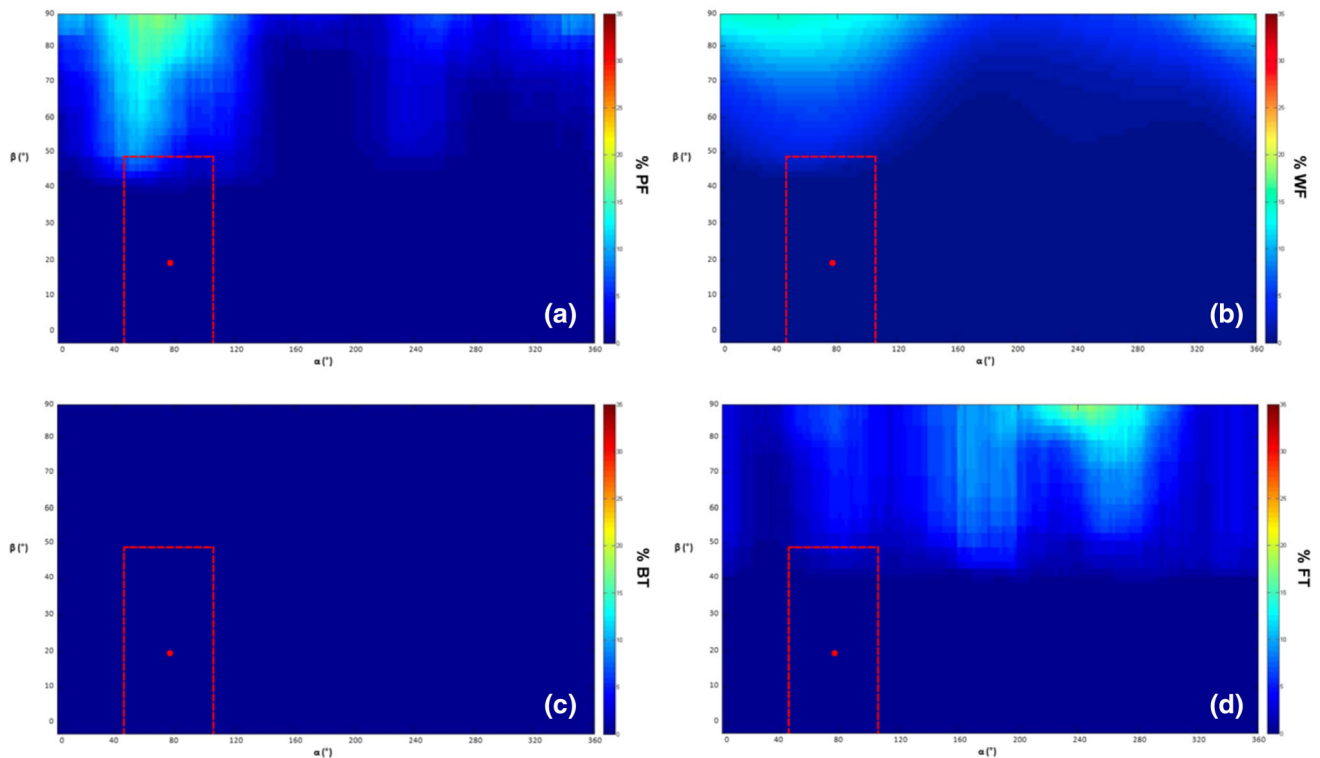


Fig. 10 Global kinematic analysis results, considering each possible slope dip and dip direction value (varying from 0° to 90° and 0° to 360° , respectively, along an array with interval of 1°), for the different analysed failure mechanisms: **a** plane failure, **b** wedge failure, **c** block

toppling, **d** flexural toppling. For each mechanism, the average slope orientation (*red dot*) and scatter (*red dashed rectangle*) are indicated (colour figure online)

The quality of the rock mass in front of the Costa Concordia cruise ship was classified as good based on the geomechanical characterization according to the Barton et al. (1974), Bieniawski (1989) and Hoek et al. (1995) criteria. More generally, the rock mass featured both intact areas (sector A, Fig. 5) and intensely jointed areas (sector B, Fig. 5). The global compressive strength (σ_{cm}) of the rock mass in each sector was much lower than the compressive strength of undisturbed rock samples ($\sigma_c = 113.51$ MPa), highlighting the influence of discontinuities and alteration of the rock surfaces.

To completely characterize the rock mass quality in Cala Lazzaretto and Punta Gabbianara, seismic refraction and geoelectric campaigns were also performed. The P-wave seismic refraction survey (Fig. 6) highlighted a surficial level (4–8 m) of low rock quality; below this level, the results showed good and very good quality. These results confirm the low resistance (σ_c) values obtained from point load tests for the surficial altered level with respect to literature values for intact rock resistance. At depth of 4–8 m below the surface, this value should be close to the literature value (approximately 150 MPa, i.e., Hansen 1988; Hoek and Brown 1980).

Moreover, the geoelectric survey results (Fig. 6) showed the variability of the rock conductivity in the surficial level,

highlighting different degrees of fracturing in the investigated rock mass. The orientation of the recognized discontinuities was compatible with the lineations recognized in the non-stereoscopic digital orthophotos and with the discontinuity sets identified by the semiautomatic and traditional surveys. In particular, set JN3 was clearly recognizable, even in the orthophotos.

The manually and semiautomatically collected features, together with the reconstruction of the three-dimensional surface, were used to perform 3D and global kinematic analysis of the main failure mechanisms using the program DiAna-K (Gigli et al. 2012a). These analyses qualitatively and quantitatively assessed the spatial distribution of instability mechanisms. The highest kinematic hazard index value was predominantly associated with the plane failure (PF) and flexural toppling (FT) mechanisms, being concentrated in Cala del Lazzaretto and nearby Punta Gabbianara, respectively (Fig. 9a, d). The risk linked to these mechanisms was also present on the seabed underlying the cruise ship, but the index values did not exceed 6%. The global kinematic analysis (Fig. 10), in particular, indicated that the risk of failure of the rocky spur was very low. Wedge failure and direct toppling were almost absent.

The highest index value reached 12% (3D analysis), suggesting low spatial failure risk.

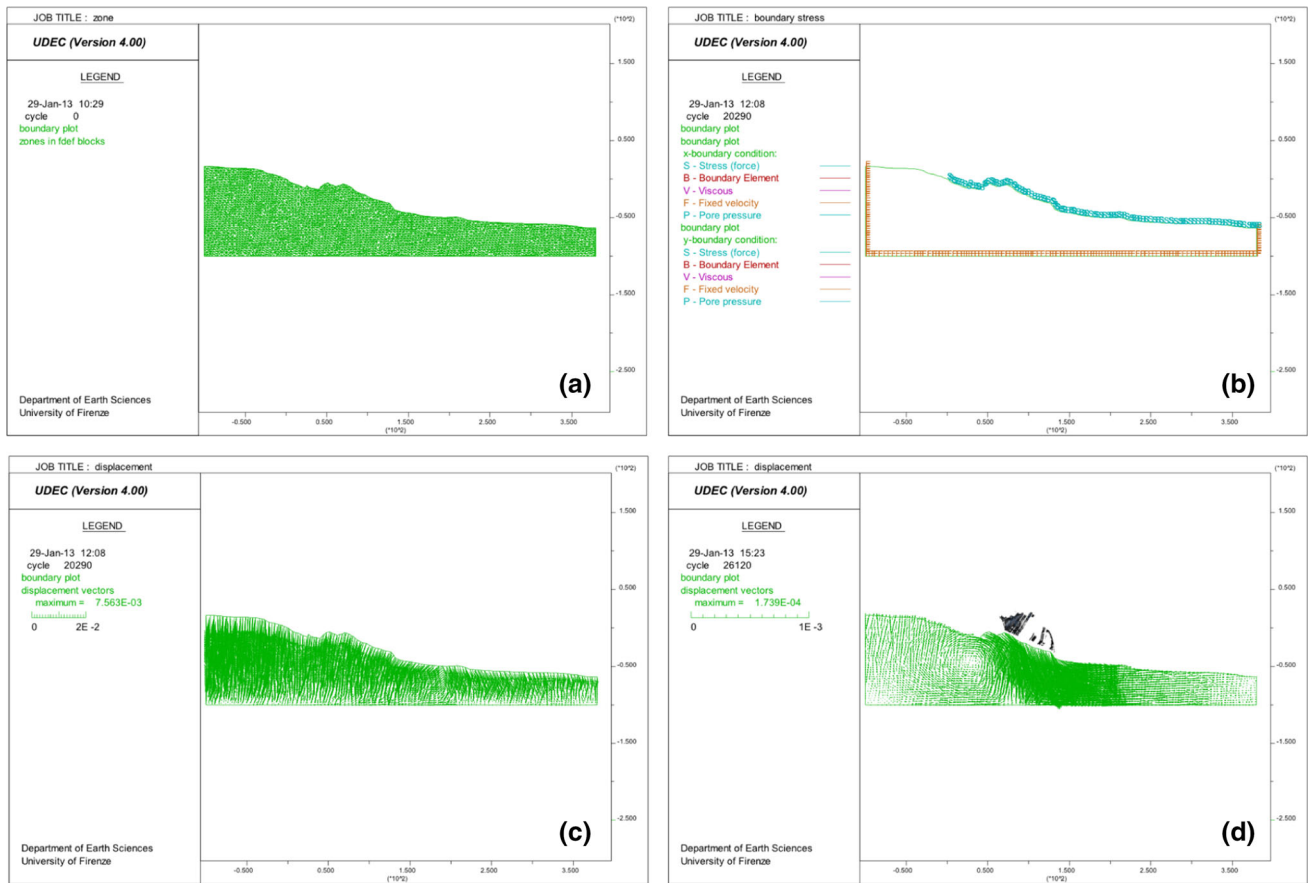


Fig. 11 Numerical modelling results: **a** initial model, **b** boundary condition and water table (third step), **c** displacement vectors (shipwreck load not considered), **d** displacement vectors and plastic deformation (shipwreck load considered)

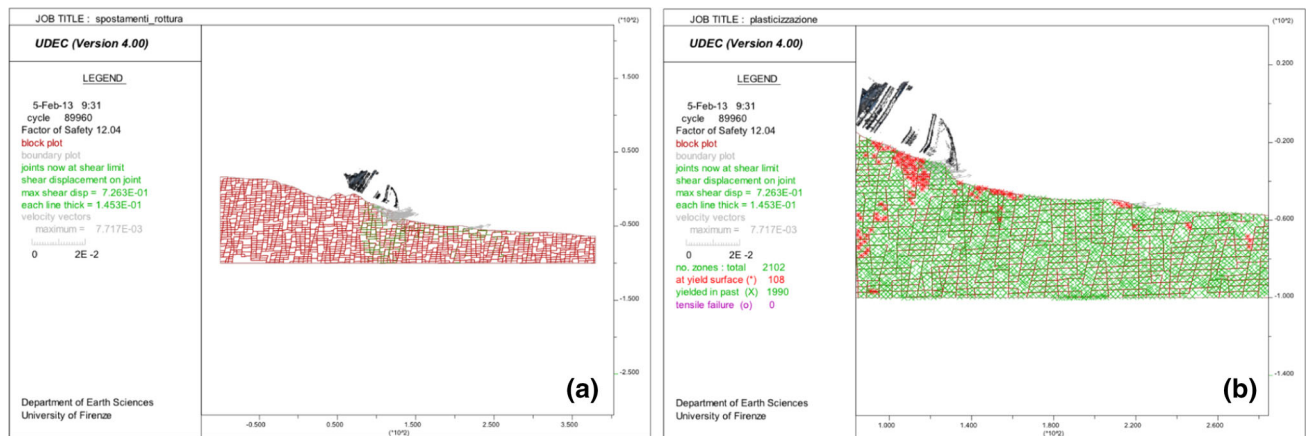


Fig. 12 Numerical modelling results: **a** shear displacement on joints (green lines) with shipwreck load considered, **b** plastic deformation (red lines) with shipwreck load considered (colour figure online)

Comparing the spatial distribution of the kinematic indexes (Fig. 9) with the distribution of the rock mass slope and aspect in the 3D mesh (Fig. 8), the main set involved in the instability mechanisms is the medium-dip-angle set JN4, as confirmed by the global kinematic analysis.

Using the distinct element method numerical model (UDEC, Itasca 2004), a stability analysis was performed along a profile representing the worst possible scenario.

The displacement vector plot (Fig. 11d) shows that the highest displacement values are millimetric. Additionally, the safety factor confirms the general stability of the rock

mass ($F = 12$, Fig. 12a). Plastic deformation is concentrated on the rocky cliff where the ship is located (Fig. 12b), and the highest estimates of the shear displacement on the joints are on the order of a few decimetres.

Despite the unfamiliarity of the scenario, the presented study represents a successful combination of both traditional and TLS surveys carried out to support stability analysis in a unique operational setting.

Furthermore, in the framework of disaster management and civil protection, the data obtained from the employed monitoring systems were perfectly integrated.

Acknowledgements This research was funded by the Italian National Department of Civil Protection (DPC), under agreement OPCM 3998/2012 “Monitoring of the deformations and displacements of the Costa Concordia cruise ship (Giglio Island, GR)”. The authors thank Luca Tanteri, Veronica Pazzi and William Frodella (Earth Science Department of the University of Florence) for the field survey and laboratory tests. We are grateful to the National Institute of Oceanography and Experimental Geophysics (OGS) for the high-precision bathymetric survey data from the Punta Gabbianara seabed.

Open Access This article is distributed under the terms of the Creative Commons Attribution 4.0 International License (<http://creativecommons.org/licenses/by/4.0/>), which permits unrestricted use, distribution, and reproduction in any medium, provided you give appropriate credit to the original author(s) and the source, provide a link to the Creative Commons license, and indicate if changes were made.

References

- Abellan A, Vilaplana JM, Martinez J (2006) Application of a long-range terrestrial laser scanner to a detailed rockfall study at Vall de Nuria (Eastern Pyrenees, Spain). *Eng Geol* 88:136–148
- Abellan A, Calvet J, Vilaplana JM, Blanchard J (2010) Detection and spatial prediction of rockfalls by means of terrestrial laser scanner monitoring. *Geomorphology* 119(3–4):162–171. doi:10.1016/j.geomorph.2010.03.016
- Barton NR (1973) Review of a new shear strength criterion for rock joints. *Eng Geol* 7:287–332
- Barton N, Choubey V (1977) The shear strength of rock joints in theory and practice. *Rock Mech* 10:1–54
- Barton NR, Lien R, Lunde J (1974) Engineering classification of rock masses for the design of tunnel support. *Rock Mech* 6(4):189–239
- Bieniawski ZT (1989) *Engineering rock mass classifications*. Wiley, New York
- Blackwelder E (1925) Exfoliation as a phase of rock weathering. *J Geol* 33:793–806
- Broussolle J, Kyovtorov V, Basso M, Ferraro Di Silvi E, Castiglione G, Figueiredo Morgado J, Giuliani R, Oliveri F, Sammartini PF, Tarchi D (2014) MELISSA, a new class of ground based InSAR system. An example of application in support to the Costa Concordia. *ISPRS J Photogramm Remote Sens* 91:50–58
- Casagli N, Pini G (1993) Analisi cinematica della stabilit  in versanti naturali e fronti di scavo in roccia. *Geol Appl e Idrog* 28:223–232
- Ciampalini A, Raspini F, Bianchini S, Tarchi D, Vespe M, Moretti S, Casagli N (2016) The Costa Concordia last cruise: the first application of high frequency monitoring based on COSMO-SkyMed constellation for wreck removal. *ISPRS J Photogramm Remote Sens* 112:37–49
- Dawson EM, Roth WH, Drescher A (1999) Slope stability analysis by strength reduction. *G otechnique* 49(6):835–840
- Deere DU (1963) Technical description of rock cores for engineering purposes. *Felsmechanik und Ingenieurgeologie* 1:16–22
- Deere DU, Miller RP (1966) Engineering classification and index properties of rock. Technical Report n. AFNL-TR-65-116, Air Force Weapon Laboratory, New Mexico
- DPC (Italian National Department of Civil Protection) (2012). Indagini geologiche, geomeccaniche e geofisiche nella zona di Punta Gabbianara (Isola del Giglio). Preliminary report (in Italian), unpublished
- Eberhardt E, Stead D, Coggan JS (2004) Numerical analysis of initiation and progressive failure in natural rock slopes—the 1991 Randa rockslide. *Int J Rock Mech Min* 41(1):69–87
- Fanti R, Gigli G, Lombardi L, Tapete D, Canuti P (2012) Terrestrial laser scanning for rockfall stability analysis in the cultural heritage site of Pitigliano (Italy). *Landslides*. doi:10.1007/s10346-012-0329-5
- Ferrero AM, Forlani G, Roncella R, Voyat HI (2009) Advanced geosurvey methods applied to rock mass characterization. *Rock Mech Rock Eng* 42:631–665
- Gigli G, Casagli N (2011) Semiautomatic extraction of rock mass structural data from high resolution LIDAR point clouds. *Int J Rock Mech Min Sci* 48(2):187–198
- Gigli G, Mugnai F, Leoni L, Casagli N (2009) Brief communication “Analysis of deformations in historic urban areas using terrestrial laser scanning”. *Nat Hazards Earth Syst Sci* 9:1759–1761. doi:10.5194/nhess-9-1759-2009
- Gigli G, Frodella W, Mugnai F, Tapete D, Cigna F, Fanti R, Intrieri E, Lombardi L (2012a) Instability mechanisms affecting cultural heritage sites in the Maltese Archipelago. *Nat Hazards Earth Syst Sci* 12:1–21
- Gigli G, Morelli S, Fornera S, Casagli N (2012b) Terrestrial laser scanner and geomechanical surveys for the rapid evaluation of rock fall susceptibility scenarios. *Landslides* 11:1–14. doi:10.1007/s10346-012-0374-0
- Goodman RE (1976) *Methods of geological engineering in discontinuous rocks*. West, St. Paul
- Goodman RE (1980) *Introduction to rock mechanics*. Wiley, New York
- Goodman RE, Bray JW (1976) Toppling of rock slopes. In: *Proceeding speciality conference on rock engineering for foundations and slopes*, ASCE, Boulder (Colorado) 2, pp 201–234
- Griffiths DV, Lane PA (1999) Slope stability analysis by finite elements. *G otechnique* 49(3):387–403
- Hansen TH (1988) *Rock properties*. Norwegian tunnelling today 41–44
- Hoek E (1973) Methods for the rapid assessment of the stability of three dimensional rock slope. *Q J Eng Geol* 6:243–255
- Hoek E, Bray JW (1981) *Rock slope engineering*. Institution of Mining and Metallurgy, London
- Hoek E, Brown ET (1980) Empirical strength criterion for rock masses. *J Geotech Geoenviron* 106(GT9):1013–1035
- Hoek E, Brown ET (1997) Practical estimates of rock mass strength. *J Rock Mech Min Sci & Geomech Abstr* 34(8):1165–1186
- Hoek E, Wood D, Shah S (1992) A modified Hoek–Brown failure criterion for jointed rock masses. In: *Proceedings of international conference on Eurock’92*, Chester, England, pp 209–214
- Hoek E, Kaiser PK, Bawden WF (1995) Support of underground excavations in hard rock. A. A. Balkema, Rotterdam
- Hoek E, Caranza-Torres C, Corkum B (2002) *Hoek and Brown criterion 2002 Edition*. In: *Proceeding NARMS-TAC conference*, Toronto, 1, pp 267–273

- Hudson JA, Harrison JP (1997) Engineering rock mechanics: an introduction to the principles and applications. Pergamon, Oxford
- ISRM (1978) Commission on the standardization of laboratory and field test. Suggested methods for the quantitative description of discontinuities in rock masses. *Int J Rock Mech Min* 15(6):319–368
- ISRM (1985) Suggested methods for determining point load strength. *Int J Rock Mech Min* 22(2):51–62
- Itasca (2004) UDEC: universal distinct element code—version 4. User's manual. Itasca Consulting Group Inc., Minneapolis
- Jaboyedoff M, Metzger R, Oppikofer T, Couture R, Derron MH, Locat J, Durmel D (2007) New insight techniques to analyze rock-slope relief using DEM and 3D- imaging cloud points: COLTOP-3D software. In: Eberhardt E, Stead D, Morrison T (eds) *Rock mechanics: meeting society's challenges and demands*. Taylor & Francis Group, London, pp 61–68
- Jaboyedoff M, Couture R, Locat P (2009) Structural analysis of Turtle Mountain (Alberta) using digital elevation model: toward a progressive failure. *Geomorphology* 103:5–16
- John KW (1968) Graphical stability analysis of slopes in jointed rock. *J Soil Mech Found Div* 94(SM2):497–526
- Johnston IW (1993) Soft rock engineering. *Comprehensive rock engineering* 1:367–393
- Lato M, Diederichs MS, Hutchinson DJ, Harrap R (2009) Optimization of LiDAR scanning and processing for automated structural evaluation of discontinuities in rock masses. *Int J Rock Mech Min* 46:194–199
- Lato M, Diederichs M, Hutchinson DJ (2010) Bias correction for static LiDAR scanning of rock outcrops for structural characterization. *Rock Mech Rock Eng* 43(5):615–628
- Lombardi L, Casagli N, Gigli G, Nocentini M (2006) Verifica delle condizioni di sicurezza della S.P. Lodovica in seguito ai fenomeni di crollo nella cava di Sesto di Moriano (Lucca). *G Geol Appl* 3:249–256 (in Italian)
- Marinos P, Hoek E (2001) Estimating the mechanical properties of heterogeneous rock masses such as flysch. *Bull Eng Geol Environ* 60:85–92
- Marinos P, Marinos V, Hoek E (2004) Geological Strength Index, GSI: applications, recommendations, limitations and alteration fields commensurately with the rock type. *Bulletin of the Geological Society of Greece*, vol 36—proceedings of the 10th international congress, Thessaloniki
- Markland JT (1972) A useful technique for estimating the stability of rock slopes when the rigid wedge sliding type of failure is expected. *Imperial College Rock Mechanics Research Report* 19
- Matheson GD (1983) Rock stability assessment in preliminary site investigations—graphical methods. *Transport and Road Research Laboratory Report* 1039
- Matheson GD (1989) The collection and use of field discontinuity data in rock slope design. *Q J Eng Geol Hydrogeol* 22:19–30
- Oppikofer T, Jaboyedoff M, Blikra L, Derron MH, Metzger R (2009) Characterization and monitoring of the Aknes rockslide using terrestrial laser scanning. *Nat Hazards Earth Syst Sci* 9:1003–1019
- Rahman Z, Slob S, Hack R (2006) Deriving roughness characteristics of rock mass discontinuities from terrestrial laser scan data. In: Culshaw MG, Reeves HJ, Jefferson I, Spink TW (eds) 10th international congress IAEG 2006: engineering geology for tomorrow's cities, Nottingham, UK, 6–10 September 2006. Geological Society of London, London, UK, Paper 437
- Raspini F, Moretti S, Fumagalli A, Rucci A, Novali F, Ferretti A, Prati C, Casagli N (2014) The COSMO-SkyMed constellation monitors the Costa Concordia wreck. *Remote Sens* 6:3988–4002
- Rocscience (2004) Roclab. www.rocscience.com
- Russo G, Kalamaras S, Origlia L, Grasso P (2001) A probabilistic approach for characterizing the complex geological environment for design of the new metro of Porto. AITES-ITA 2001 World Tunnel Congress, Milano, pp 463–470
- Schröder-Hinricks J, Hollnagel E, Baldauf M (2012) From Titanic to Costa Concordia—a century of lessons not learned. *WMU J Marit Aff* 11:151–167
- Slob S, Hack HRGK (2004) 3D terrestrial laser scanning as a new field measurement and monitoring technique. In: *Engineering geology for infrastructure planning in Europe: a European perspective*, Lecture Notes in Earth Sciences, vol 104. Springer, Berlin/Heidelberg, pp 179–190
- Slob S, Hack HRGK (2007) Fracture mapping using 3D laser scanning techniques. In: 11th congress of the international society for rock mechanics: the second half century of rock mechanics, 9–13 July 2007, Lisbon, Portugal, Taylor & Francis, Balkema
- Slob S, Hack HRGK, Turner K (2002) An approach to automate discontinuity measurements of rock faces using laser scanning techniques. In: Dinid da Gama C, Riberia e Sousa L (eds) *Proceedings of ISRM EUROCK 2002*, 25–28 November 2002, Funchal, Portugal, Sociedade Portuguesa de Geotecnia, pp 87–94
- Slob S, Hack R, Van Knapen B, Turner K, Kemeny J (2005) A method for automated discontinuity analysis of rock slopes with 3D laser scanning. *Transp Res Rec* 1913:187–208
- Sturzenegger M, Stead D (2009) Quantifying discontinuity orientation and persistence on high mountain rock slopes and large landslides using terrestrial remote sensing techniques. *Nat Hazards Earth Syst Sci* 9:267–287
- Tapete D, Gigli G, Mugnai F, Vannocci P, Pecchioni E, Morelli S, Fanti R, Casagli N (2012) Correlation between erosion patterns and rockfall hazard susceptibility in hilltop fortifications by terrestrial laser scanning and diagnostic investigations. In: *IEEE international geoscience and remote sensing symposium. Remote sensing for a dynamic earth*. Munich, Germany, 22–27 July 2012, pp 4809–4812
- Turner AK, Kemeny J, Slob S, Hack HRGK (2006) Evaluation and management of unstable rock slopes by 3-D laser scanning In: Culshaw MG, Reeves HJ, Jefferson I, Spink TW (eds) 10th international congress IAEG 2006: engineering geology for tomorrow's cities, Nottingham, UK, 6–10 September 2006. Geological Society of London, London, UK, Paper 404
- Westerman DS, Innocenti F, Tonarini S, Ferrara G (1993) The Pliocene intrusions of the Island of Giglio. *Mem Soc Geol Ital* 49:345–363